



Contents lists available at [Egyptian Knowledge Bank](https://egyptianknowledgebank.com)

# Advances in Environmental and Life Sciences

journal homepage: <https://aels.journals.ekb.eg>



## New Terbium Complex for Detection of Gemifloxacin Mesylate in Different Samples Using Luminescence and Time Resolved Method

Rania M Goda<sup>a</sup>, Zeinab M Anwar<sup>a</sup>, Axel Duerkop<sup>b</sup>, Gasser M Khairy<sup>a, \*\*</sup>

<sup>a</sup>Chemistry Department, Faculty of Science, Suez Canal University, 41522, Ismailia, Egypt

<sup>b</sup>Institute of Analytical Chemistry, Chemo and Biosensors, Faculty of Chemistry and Pharmacy, University of Regensburg, 93053, Regensburg, Germany

### Abstract

A new optical sensing microplate was developed for rapidly determining Gemifloxacin Mesylate in its pure form, pharmaceutical preparations, and human plasma using new Tb(III)-complex with 3-allyl-2-hydroxybenzohydrazide (AZ) as a probe. The interaction of Gemifloxacin mesylate with the Tb (III)- (AZ)<sub>2</sub> complex is based on the luminescence enhancement. The metal to ligand ratio of the complex is 1:2 as determined by a Job plot method. The calibration graph was linear over the range of 0.15–10 µg/mL, with a limit of quantification (LOQ) of 0.15 µg/mL and a detection limit (LOD) of 0.05 µg/mL. The thermodynamic analysis for the interaction GMF with Tb (III)-(AZ)<sub>2</sub> complex was evaluated. The thermodynamic analysis showed that the interaction between the Tb (III)-(AZ)<sub>2</sub> complex and GMF was spontaneous with negative ΔG. The established approach has been used successfully to the determination of drugs in pharmaceutical formulations and spiked plasma samples with good recovery percent and RSD less than five percent.

**Keywords:** Probe, Lanthanide complex, Gemifloxacin mesylate, Luminescence, Time resolved

### 1. Introduction

The fluoroquinolone antibiotic known as gemifloxacin mesylate (GMF) is a fourth-generation fluoroquinolone with enhanced affinity for bacterial topoisomerase IV. It is currently in the process of being developed as a treatment for mild-to-moderate pneumonia, acute exacerbations of chronic bronchitis, and urinary tract infections. This substance has action against a wide variety of bacteria, including Gram-positive as well as Gram-negative bacteria. The bactericidal effect of gemifloxacin is due to the drug's ability to block the enzymes topoisomerase II (DNA gyrase) and topoi-

somerase IV. These enzymes are necessary for the replication, transcription, repair, and recombination of bacterial DNA [1].

As a consequence of this, a variety of analytical techniques have been published for the quantification of GFM in pharmacological formulations or biological fluids such as high-performance liquid chromatography (HPLC) [2–5], high-performance liquid chromatography–tandem mass spectrometry (LC–MS–MS) [6–8], capillary electrophoresis [9], and voltammetry [10, 11]. However, these methods have some drawbacks such as time consuming, tedious, and dedicated to sophisticated and required expensive instruments. Also, they lack simplicity of the assay procedure (e.g., heating, or liquid-liquid extraction steps) which required trained person.

As a result, a method of analysis that is not only straightforward but also fast and sensitive is re-

\* Corresponding author.

Email address:

[gasser\\_mostafa@science.suez.edu.eg](mailto:gasser_mostafa@science.suez.edu.eg) (Gasser M Khairy)

doi [10.21608/AELS.2023.205300.1032](https://doi.org/10.21608/AELS.2023.205300.1032)

Received: 1 May 2023, Revised: 10 May 2023  
Accepted: 14 May 2023, Published: 1 July 2023

quired in order to routinely analyze gemifloxacin mesylate (GMF) in its many different pharmaceutical dose forms. These criteria may be satisfied using chemosensors. As compared to alternative methods, utilizing chemosensors has a number of advantageous qualities. Because of the way the molecules are designed, optical chemosensors that make use of photoluminescence have the potential to deliver excellent selectivity in addition to great sensitivity. In addition to this, it is possible to achieve lower detection limits due to the fact that the detected signal is proportional to both the concentration of the analyte and the intensity of the excitation source. This is in contrast to photometry, in which the negative log of a signal ratio is proportional to the concentration of the analyte. Hence, it is possible to achieve both a quick response and real-time monitoring in actual samples if a chemosensor (or probe) is used that has an appropriate binding constant, high molar absorbance, and high quantum yield. Spectrofluorimetric approaches have emerged as the method of choice for evaluating a wide range of pharmaceuticals in a variety of dosage forms as well as biological samples. This is due to the fact that spectrofluorimetric methods are now carried out in a high-throughput microtiter plate format, in which 96 or more samples can be detected within minutes. This improves reproducibility through the testing of multiple replicates of each sample [12, 13].

Luminescent lanthanide complexes are suited for use as optical sensors as a result of their exceptional qualities. These properties include lengthy luminescence lifetimes on the order of milliseconds, huge Stoke's shifts, relatively strong quantum yields, and a high coordination number that allows them to form even ternary complexes. There is a substantial difference between lanthanide complexes and other organic molecules due to the presence of f-f forbidden transitions, which is another characteristic of lanthanide complexes. They are capable of displaying narrow emissions and a high degree of color purity. In addition, there are a few more distinctive qualities that may be found in materials based on Ln, which will be discussed as follows: Antenna effect Indirect excitation, also known as sensitization or the antenna effect, is one

of the significant characteristics that may be found in Ln-based materials. Indirect excitation is also one of the names of this phenomenon. This process takes place in three stages: first, appropriate organic molecules called chromophores that are connected to the Ln ion absorb excitation light; second, energy is transferred from the ligand to one or many excited states of the Ln ion; and last, the Ln ion emits light. For the purpose of accomplishing this goal, a number of organic ligands that include aromatic chromophores have been used. To chelate with lanthanide ions and operate as an antenna to transmit its emission energy to the lanthanide ion, gemifloxacin mesylate (GMF) with keto-acid functionality might be used [14, 15].

As a result, luminescent probes are the optimal option due to their many advantageous properties, including their high sensitivity, high selectivity, rapid response, and direct detection [16]. According to Lehn [17], lanthanide compounds with organic molecular structures exhibit fascinating photophysical characteristics, which qualify them to be employed as light conversion molecular devices. These qualities qualify lanthanide complexes to be used as light conversion molecular devices (LCMDs). The development of effective lanthanide complexes has emerged as an important research objective, which is being pursued by a number of organizations [18–23]. Several luminescent lanthanide chelates are useful alternatives to traditional fluorophores as probes [24]. Saturated green emission from Terbium complexes has attracted more attention because of the strong fluorescence emitted from the f-f hypersensitive transition, which has a large Stokes shift between the emission and excitation wavelengths (minimizing the overlap of excitation and emission spectra) and a long lifetime [25].

In this work, we sought to develop a high-throughput sensing microplate for the quantitation of GMF in pharmaceutical formulations (based on the interaction of terbium- 3-allyl-2-hydroxybenzohydrazide with GMF) as a rapid screening tool prior to other more time-consuming methods. The overall concentration of GMF was measured in one human plasma sample taken from a healthy volunteer as well as in three com-

mercially available pharmaceutical formulations (Floxguard, Quinabiotic, and Gemionce). The novel sensor plate makes it possible to detect GMF in parallel and quickly (96 samples in two minutes) using fluorescence equipment that is already in use. Also, the sensing plate allows time-saving parallelized sample preparation across 8–12 channels, which adds to a rigorous statistical assessment of the fluorescence measurement. For the purpose of performing regular quality control checks on pharmaceutical formulations using relatively low-priced apparatus, the suggested approach is simple, sensitive, trustworthy, and quick.

## 2. Material and methods

### 2.1. Materials and solutions

Terbium chloride hexahydrate ( $\text{TbCl}_3 \cdot 6\text{H}_2\text{O}$ ) was purchased from Sigma–Aldrich ([www.sigmaaldrich.com](http://www.sigmaaldrich.com)). Pharmaceutical grade Gemifloxacin mesylate (GMF) was supplied by EGPI company ([www.egyptiangroup.net](http://www.egyptiangroup.net)). The used ligand was: 3-allyl-2-hydroxybenzohydrazide (HAZ) was purchased from Alfa Aesar ([www.alfa.com](http://www.alfa.com)) The chemical structures of ligand and antibiotic are given in scheme S1 (see supplementary material). All solvents used were of analytical grade. All pharmaceutical drugs were obtained from commercial sources in the local markets. Floxguard tablets were obtained from Al-Debeiky Pharma. For Advocate Pharmaceuticals Company, Egypt labeled to contain 320 mg GMF per tablet. Quinabiotic tablets were obtained from Future Pharmaceutical Industries for Utopia Pharma. Gemionce tablets were obtained from Next Pharma, Egypt, labeled to contain 320 mg GMF per tablet.

The stock solutions were prepared as follows: The terbium chloride was prepared by dissolving 37.7 mg of  $\text{TbCl}_3 \cdot 6\text{H}_2\text{O}$  in 100 ml in doubly distilled water to give a final concentration of  $10^{-3} \text{ mol L}^{-1}$ .  $10^{-3} \text{ mol L}^{-1}$  of HAZ was prepared by dissolving 19.2 mg of solid ligand in 100 ml ethanol. Two Stock solutions of GMF were prepared: the first one is 1000  $\mu\text{g/mL}$  of Gemifloxacin mesylate (GMF) which was prepared for microtiter plate measurements by dissolving 10 mg in 10 ml of methanol. Another stock solution of GMF was prepared by

adding 4.85mg of GMF in 10 ml volumetric flask, and complete with methanol to get  $10^{-3} \text{ mol/L}$  of GMF for luminescence measurements. The two stock solutions of GMF were then sonicated for 10 minutes and were stored in refrigerator in well closed dark glass bottle Stock solution of GMF is usually stored at  $4^\circ\text{C}$  and kept in the dark, it was found to be stable for 2 weeks. Because of the light sensitivity of the fluoroquinolones, it stored and protected from light until assay, in amber flasks or/and covered with aluminum foil [26].

The working solutions of GMF were prepared by transferring (10, 20, 30, 50, 70, 80, 90 and 100  $\mu\text{L}$ ) of 1000  $\mu\text{g/mL}$  GMF stock solution to 10.0 ml volumetric flasks which contain 100 $\mu\text{L}$  of Tb(III) and 200 $\mu\text{L}$  of (HAZ) then completing the volume to 10 ml with methanol in order to obtain GMF concentrations of (1, 2, 3, 5, 7, 8, 9, 10 $\mu\text{g/mL}$ ), respectively.

### 2.2. Instruments

Luminescence time-resolved measurements were performed with a FLUOstar Optima microtiter plate reader (from BMG LABTECH, Offenburg, Germany, [www.bmglabtech.com](http://www.bmglabtech.com)). The instrument is equipped with the high energy xenon flash lamp. The UV-VIS spectra were acquired on a Shimadzu UV-1800 UV/Visible Spectrophotometer (<https://www.shimadzu.com>) in quartz cells with 1.00 cm path length. The luminescence spectra were recorded with a Jasco 6300 spectrofluorometer (<https://jascoinc.com>) with quartz cells of 1.00 cm path length and a 150 W xenon lamp for excitation. The excitation/emission bandwidths were 5 nm. Microtiter plates (no. 655101, 96 well microtiter plates, F-bottom) from Greiner bio-one ([www.gbo.com](http://www.gbo.com)) were used.

### 2.3. Sample preparation

To prepare the real samples from pharmaceutical formulations, the contents of ten tablets (Floxguard, Quinabiotic, or Gemionce) labeled to contain 320 mg GMF per tablet were crushed, powdered, and weighted out. An accurate weight equivalent to 10 mg GMF was transferred into a 100 mL volumetric flask, was dissolved in 60 mL methanol, kept in an ultrasonic bath for 10 min and

finally was filtered. The filtrate solution was completed to 100.0 mL with methanol.

In order to get a sample of plasma, a healthy volunteer had five milliliters of their blood taken into a tube that contained heparin, which acts as an anticoagulant. This experiment was given the go-ahead after receiving the blessing of the ethical committee of Suez Canal University. In order to separate the plasma, the tube was centrifuged for ten minutes at a speed of 9400 g. One milliliter of human plasma that had been isolated was combined with one milliliter of methanol. After that, the mixture was spun in a centrifuge at 9400 g for half an hour. The probe was used for the analysis after the supernatant was separated and collected for further study.

#### 2.4. Quantification of GMF

For time-resolved measurements, 150  $\mu\text{L}$  of each of the working standard solutions (section 2.1) were put into each well of a sensing microtiter plate to measure the amount of GMF. For Tb (III), the measurement was carried out with a FLUOstar Optima microtiter plate reader at excitation wavelengths of 320 nm and emission wavelengths of 545 nm. It was decided to have the incubation period last for 5 minutes, and it is advised that you shake the container for 5 seconds both before and after the incubation period. It was decided that the temperature should be kept at 25°C. The values of 2600 were chosen to serve as the gain settings for the microtiter plate reader. The mean fluorescence intensity was determined by taking the average of five separate observations of each concentration of GMF. These measurements were performed independently.

A standard addition method was used for measuring the amount of GMF in pharmaceutical formulation and human plasma. Increasing amount of GMF (0, 3, 5, and 7  $\mu\text{g}/\text{ml}$ ) were introduced to a volumetric flask that contained a fixed concentration (10  $\mu\text{M}$ ) of Tb (III)-(AZ)<sub>2</sub> probe and 100  $\mu\text{L}$  of the extracted sample then completing the volume to 10.0 mL with methanol. 150  $\mu\text{L}$  of each above prepared solutions with five replicates were transferred into the microtiter plate. Then, the plate has been measured as mentioned above.

### 3. Results and discussion

#### 3.1. Interaction of Tb (III) with 3-allyl-2-hydroxybenzohydrazide (HAZ)

##### 3.1.1. UV-vis spectroscopy

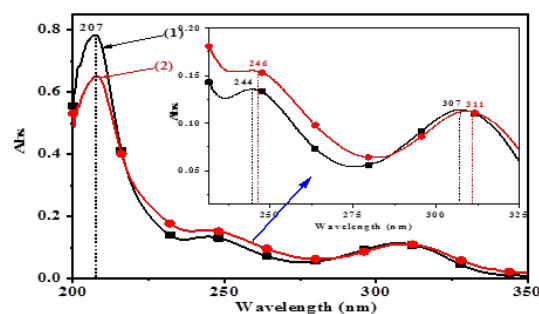


Figure 1: Absorption spectra of (1)  $2 \times 10^{-5}$  M HAZ and (2)  $1 \times 10^{-5}$  M Tb(III)-(AZ)<sub>2</sub> in methanol at room temperature

The interaction of Tb(III) with 3-allyl-2-hydroxybenzohydrazide (HAZ) has been studied using UV-vis spectroscopy. The absorption spectrum of HAZ in methanol shows three absorption bands around 207 nm and 244 nm due to the  $\pi-\pi^*$  transitions and at 307 nm due to the  $n-\pi^*$  transition as outlined in Figure (1). The extinction coefficients were  $\epsilon_{207}=(39000 \pm 400) \text{ L mol}^{-1} \text{ cm}^{-1}$ ,  $\epsilon_{244}=(7000 \pm 300) \text{ L mol}^{-1} \text{ cm}^{-1}$ , and  $\epsilon_{307}=(5500 \pm 400) \text{ L mol}^{-1} \text{ cm}^{-1}$ .

The addition of a solution of Tb(III) to the HAZ solution slightly decreases the absorbance at 207 nm, enhances the absorbance at 244 nm and red shifts the band at 307 nm to 311 nm, revealing the binding between HAZ and Tb(III) ions [27]. The extinction coefficients for the Tb(III)-(AZ)<sub>2</sub> are  $\epsilon_{207}=(65000 \pm 200) \text{ L mol}^{-1} \text{ cm}^{-1}$ ,  $\epsilon_{246}=(16000 \pm 200) \text{ L mol}^{-1} \text{ cm}^{-1}$ , and  $\epsilon_{311}=(11000 \pm 300) \text{ L mol}^{-1} \text{ cm}^{-1}$ .

The stability of Tb (III) complex in methanol at room temperature was monitored by UV-vis spectroscopy for several weeks. Liberation of the ligand was not observed under these conditions. This suggests that the complex is stable under the condition studied.

##### 3.1.2. Luminescence spectroscopy

The effect of solvents on the luminescence intensity of Tb(III)-(AZ)<sub>2</sub> complex was studied in five

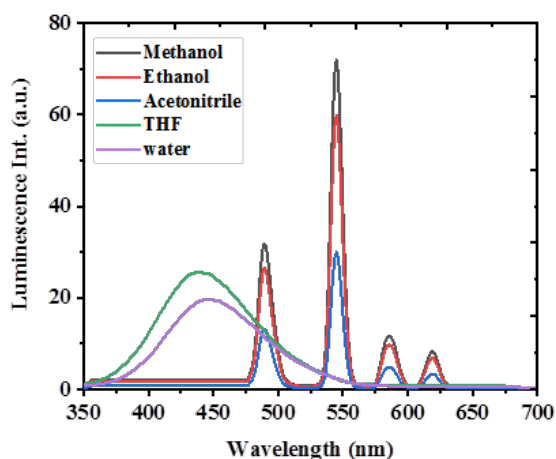


Figure 2: Fluorescence spectra of  $1.00 \times 10^{-5}$  mol/L Tb(III)-(AZ)<sub>2</sub> at  $\lambda_{exc}=307$  nm in different solvents at room temperature

different solvents. The result obtained is shown in Figure (2). All characteristic Tb(III) bands appeared at 490 nm, 545 nm, 585 nm, and 621 nm, respectively and corresponded to Tb(III) f-f transitions  $^5D_4 \rightarrow ^7F_6$ ,  $^5D_4 \rightarrow ^7F_5$ ,  $^5D_4 \rightarrow ^7F_4$  and  $^5D_4 \rightarrow ^7F_3$  respectively. These were observed in methanol, ethanol, and acetonitrile, while in water and THF, the characteristic bands of Tb(III) did not appear, but the characteristic band of ligand did appear at 445 nm. Water is a strong quencher to Tb(III) emission due to the high frequency vibrational modes of O-H oscillators. Tb(III)-(AZ)<sub>2</sub> exhibits the highest emission intensity at 545 nm in methanol. The emission of a lanthanide complex depends on the energy gap between the triplet level of the ligand and the emission level of the lanthanide ion, which sequentially impacts the efficiency of the intramolecular energy transfer from ligand to the lanthanide metal ion. In methanol, this energy gap is lowest, while non-radiative energy transfer to water is a well-known major source of the quenching of lanthanide emission in water [28]. The presence of the organic ligand (AZ), which sensitizes Tb(III) by absorbing energy and transferring it to the Tb(III) ion, which then emits the distinctive luminescence pattern of Tb(III) ions, is suggested by the clear emission intensity of Tb(III) ion at 545 nm in the presence of the ligand (AZ). The 4f-4f transitions in Tb(III) ions are parity forbidden (La-

porte rule), but they exhibit weak intensity in their absorption and emission spectra. The population of the excited states of the Tb(III) ions, however, may be increased by coordination to organic ligands like AZ<sup>-</sup>, which act as sensitizers or so-called "antennas".

### 3.1.3. The stoichiometry of probe

A Job plot was used to determine the stoichiometry of the complex formed between Tb(III) and HAZ [29, 30]. First, a series of mixtures with varying mole fractions of HAZ and Tb(III) ion were prepared, and the luminescence intensity of each mixture was determined. Then, a Job plot was constructed, as illustrated in Figure (S1 a). It is obvious from the plot that the maximum intensity of the luminescence occurs at a mole fraction of 0.37 of Tb(III). This finding reveals that one Tb(III) ion forms a complex with two molecules of HAZ, expressed as Tb(III)-(AZ)<sub>2</sub>. According to the antenna theory [31], the emission of Tb(III) is enhanced by increasing the concentration of HAZ until the molar ratio [HAZ] / [Tb(III)] = 2:1, thus suggesting the formation of Tb(III)-(AZ)<sub>2</sub> complex. By increasing the concentration of HAZ further, the emission intensity of Tb(III) is quenched by excess ligand molecules. The proposed structure of the complex in methanol is illustrated in Figure (S1 b).

## 3.2. Gemifloxacin mesylate interaction with the Tb(III)-(AZ)<sub>2</sub> probe

### 3.2.1. Uv-Visible absorption and luminescence spectroscopy of Tb(III)-(AZ)<sub>2</sub> with Gemifloxacin mesylate

The interaction of Tb(III)-(AZ)<sub>2</sub> with GMF has been studied using UV-vis spectroscopy as Figure (3). GMF shows two absorption bands at (270 and 340 nm). Upon interaction with the Tb(III)-(AZ)<sub>2</sub> probe, a blue shift was observed for the absorption bands of GMF (from 270 nm to 266 and from 340 nm to 338 nm). The mixed Tb(III)-(AZ)<sub>2</sub>-GMF complex shows an enhancement of the absorbance at four bands (207 nm, 266 nm, 319 nm, and 338 nm, respectively) compared to other systems. This reveals the binding between the complex and the additional ligand (GMF) and forming a new mixed complex of Tb(III)-(AZ)<sub>2</sub>-GMF complex [32, 33]

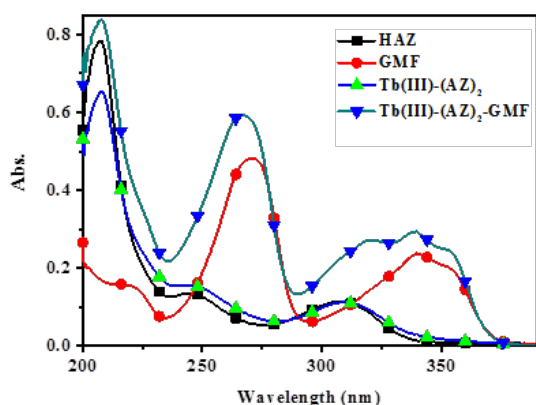


Figure 3: UV-vis spectra of  $1 \times 10^{-5}$  M Tb(III)-(AZ)<sub>2</sub> with  $1 \times 10^{-5}$  M GMF in methanol at room temperature

The extinction coefficients were  $\epsilon_{207} = (84000 \pm 400)$  L mol<sup>-1</sup> cm<sup>-1</sup>,  $\epsilon_{266} = (59000 \pm 300)$  L mol<sup>-1</sup> cm<sup>-1</sup>,  $\epsilon_{319} = (27400 \pm 400)$  L mol<sup>-1</sup> cm<sup>-1</sup> and  $\epsilon_{338} = (29800 \pm 400)$  L mol<sup>-1</sup> cm<sup>-1</sup>.

Figure (4) shows the emission spectra of  $1 \times 10^{-5}$  M Tb(III)-(AZ)<sub>2</sub> probe in the absence and presence of GMF. GMF contains a  $\beta$ -keto-acid functionality that could chelate with lanthanide ions and act as an antenna to transfer its emission energy to the lanthanide ion. This sensitized emission with a large Stokes' shift and narrow emission band in the longer wavelength region is expected to enable us to detect GMF in biological samples without any sample preparation or pretreatment procedures. Upon addition of GMF into a solution of Tb-(AZ)<sub>2</sub> probe, the four intense bands of terbium were observed, with a maximum peak at 545 nm (<sup>5</sup>D<sub>4</sub> → <sup>7</sup>F<sub>5</sub> transition). Importantly, the native fluorescence of the GMF molecule drastically decreased in the presence of Tb-(AZ)<sub>2</sub> probe and suggests an efficient excitation energy transfer from GMF to Tb(III) (Figure 4). It was observed that Tb(III) alone, upon chelation with GMF, also shows the sensitized emission of the terbium emission but the emission is higher than the case of Tb(III)-(AZ)<sub>2</sub> complex with GMF (Figure 4).

These results show the significance of using the special ligand (HAZ) for Tb(III) in the sensitized detection of GMF [34]. The Tb(III)-(AZ)<sub>2</sub> complex has two vacant sites for coordination, which are used for binding GMF. The resultant mixed complex,

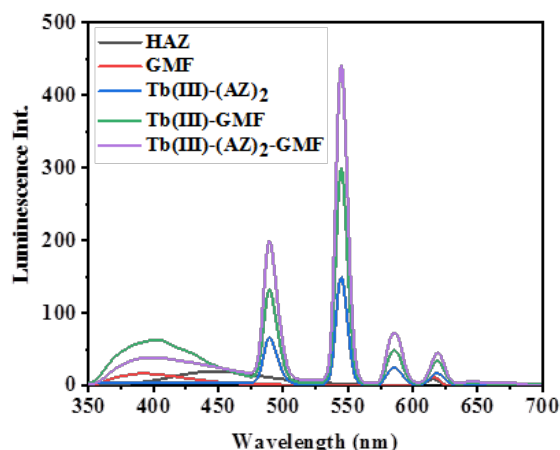


Figure 4: Luminescence spectra of Tb(III)-(AZ)<sub>2</sub>-(GMF) system at excitation wavelength 307 nm in methanol and at room temperature [Tb(III)] = [AZ]<sub>2</sub> = [GMF] =  $1 \times 10^{-5}$  M (sensitivity high)

GMF-bound Tb(III)-(AZ)<sub>2</sub>, hence, shows the best performance with enhanced sensitized emission from terbium and decreased emission from GMF (Figure 5). Importantly, the sensitized emission band is fully separated from that of GMF, which would enable us to detect GMF by using a common fluorimeter, not by resorting to the time-gated luminescence measurement function in advanced instruments.

### 3.2.2. Solvent effect on the luminescence spectra of Tb(III)-(AZ)<sub>2</sub> complex upon interaction toward GMF

Figures (S2) show the luminescence investigation of the interaction of the Tb-(AZ)<sub>2</sub> complex with GMF in various solvents. The solvents used were ethanol, methanol, tetrahydrofuran, acetonitrile, and doubly distilled water. The luminescence spectra of the probe showed four emission bands which are characteristic of Tb(III) ions at 490 nm, 545 nm, 587 nm, and 620 nm, respectively, which correspond to the <sup>5</sup>D<sub>4</sub> → <sup>7</sup>F<sub>6</sub>, <sup>5</sup>D<sub>4</sub> → <sup>7</sup>F<sub>5</sub>, <sup>5</sup>D<sub>4</sub> → <sup>7</sup>F<sub>4</sub>, and <sup>5</sup>D<sub>4</sub> → <sup>7</sup>F<sub>3</sub> transitions, respectively. The emission intensity at 545 nm showed superior emission intensity compared to those at 490 nm, 587 nm, and 620 nm. The emission bands of the Tb(III)-(AZ)<sub>2</sub> complex in the presence of GMF were acquired in ethanol, methanol, and water, while the emission bands almost disappeared in THF and

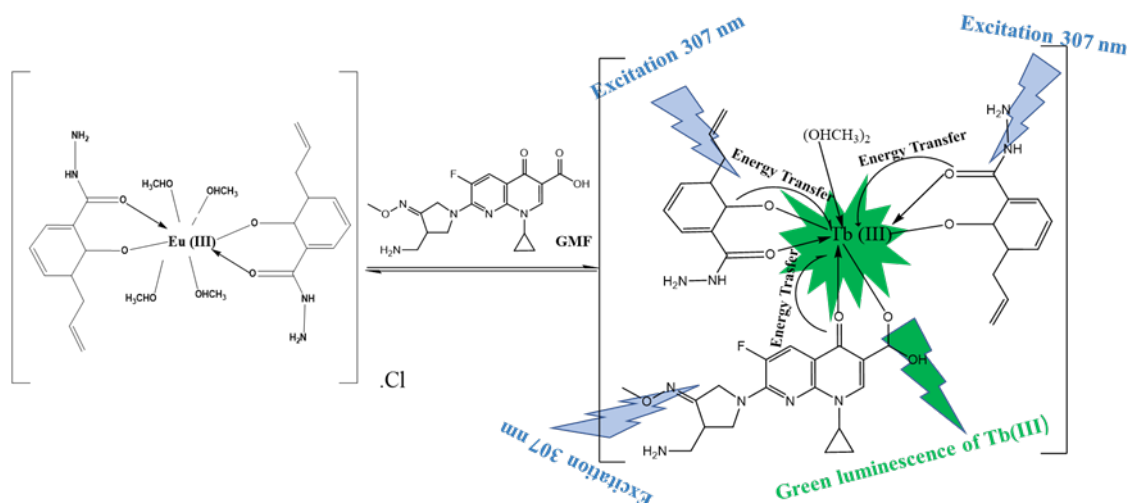


Figure 5: Proposed mechanism of GMF with Tb(III)-(AZ)<sub>2</sub>

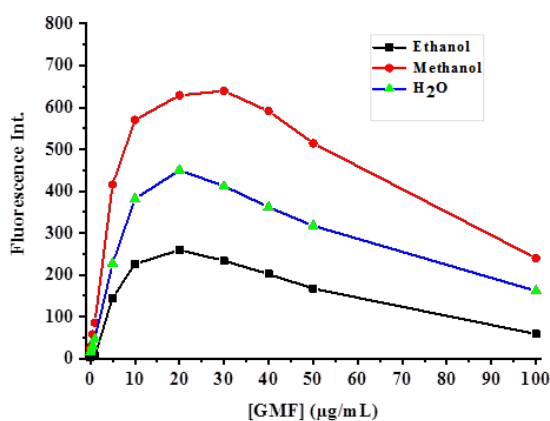


Figure 6: The interaction of  $1 \times 10^{-5}$  M Tb(III)-(AZ)<sub>2</sub> complex with different concentrations of GMF (0.01, 0.05, 0.1, 0.5, 1, 5, 10, 20, 30, 40, 50, 100  $\mu\text{g/mL}$ ) at  $\lambda_{exc/em} = 307 \text{ nm}/545 \text{ nm}$  at room temperature (sensitivity medium)

acetonitrile. The emission of a lanthanide complex depends on the energy gap between the triplet level of the ligand and the emission level of the lanthanide ion, which sequentially impacts the efficiency of the intramolecular energy transfer from the ligand to the lanthanide metal ion. In polar solvents, this energy gap is lower, while in acetonitrile and THF, this energy gap is higher which doesn't allow the energy transfer process to occur [28].

In order to determine the best solvent for the measurements of GMF using the Tb-(AZ)<sub>2</sub> complex as new probe preliminary calibration plots of the

GMF assay were obtained in water, ethanol and methanol. The emission of the Tb(III)-(AZ)<sub>2</sub> probe shows an enhancement of the characteristic peak of Tb(III) at  $\lambda_{em} = 545 \text{ nm}$  at increasing GMF concentrations, as shown in Figure (6). The plots display a narrow linear range at low concentrations of GMF. From the plots, it was noticed that the slope of the linear part of the plot obtained for methanol is the highest one. As the sensitivity of an analytical determination of GMF is related to the slope, methanol was used as the most suitable solvent for determination of GMF using the Tb-(AZ)<sub>2</sub> probe.

### 3.2.3. Effect of incubation time

Response time is the amount of time required for a sensor to respond (almost) completely to a change in input. To determine the response time, the luminescence intensity of the Tb(III)-(AZ)<sub>2</sub> complex was measured after interaction with various concentrations of GMF at 5 min to 55 min in increments of 5 min. Figure (7) illustrates that luminescence decreases at all concentrations of GMF added which stabilizes after 15 min. As we intended to develop a rapid luminescence assay for GMF and in order to keep this loss of signal small, the optimum response time for the assay was chosen to be 5 min.

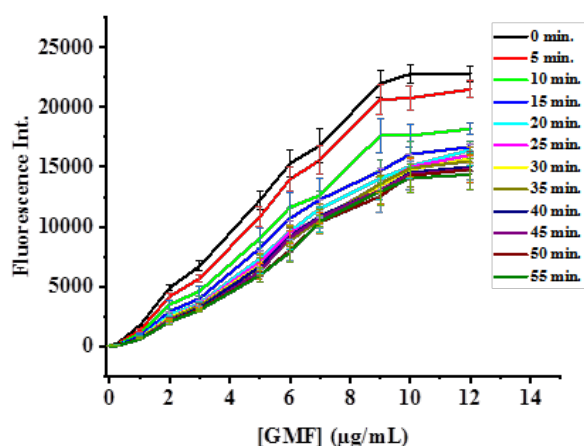


Figure 7: Plot of luminescence intensity of Tb(III)-(AZ)<sub>2</sub> at  $\lambda_{em} = 545$  nm after reaction with GMF after various incubation times

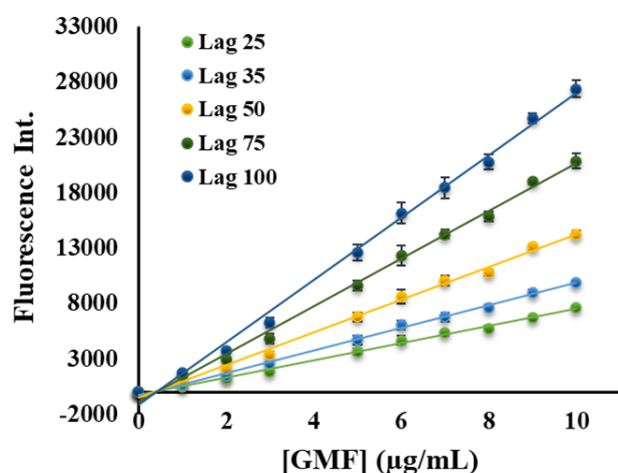


Figure 8: Effect of lag time on the luminescence intensity of the Tb(III)-(AZ)<sub>2</sub> assay for determination of GMF

### 3.2.4. Effect of lag time

Time-resolved luminescence measurements could help to reduce the fast-decaying background luminescence and the luminescence of interfering substances to get superior sensitivity for lanthanide complexes [35]. For determination of the best lag time for quantitation of GMF working solutions of  $1 \times 10^{-5}$  mol/L Tb(III)-(AZ)<sub>2</sub> complex in the presence of different concentration of GMF (between 0.5–10  $\mu\text{g}/\text{ml}$ ) were prepared and pipetted into a microtiter plate (150  $\mu\text{L}$  into each well). The intensities of luminescence were recorded us-

ing microtiter plate reader with various lag times (25, 35, 50, 75 and 100  $\mu\text{s}$ ) while the integration time was kept constant at 1000  $\mu\text{s}$  and the gain was set to 2600. Figure (8) shows the effect of lag time on the luminescence intensity of Tb(III)-(AZ)<sub>2</sub> complex in the presence of different concentration of GMF. It turns out that 100  $\mu\text{s}$  lag time is appropriate to achieve the best sensitivity for the current assay.

### 3.2.5. Binding constant and stoichiometry between Gemifloxacin mesylate and Tb(III)-(AZ)<sub>2</sub> complex

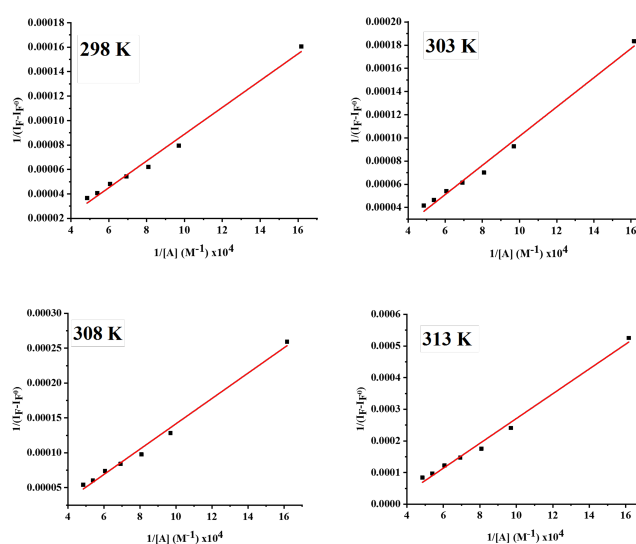


Figure 9: Benesi-Hildebrand plots for the interaction of Tb(III)-AZ<sub>2</sub> complex with different concentrations of GMF in methanol at 298 K, 303 K, 307 K and 313 K

The association constant and stoichiometry of the Tb-(AZ)<sub>2</sub> complex-GMF system were calculated by using the changes induced in the fluorescence emission spectra of the Tb-(AZ)<sub>2</sub> complex in the presence of different concentrations of GMF at various temperatures. The association constant of the formed complex (K) is given by a Benesi-Hildebrand plot [46]:

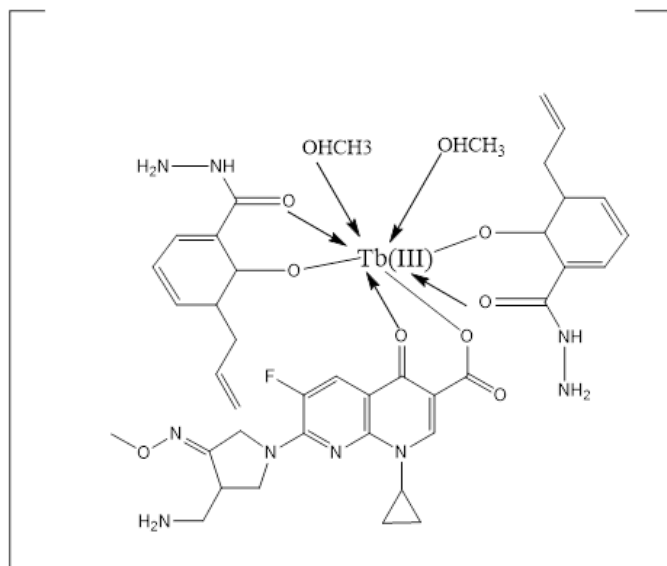
$$\frac{F^0}{F - F^0} = \alpha + \frac{\alpha}{K[A]}, \quad \alpha = \frac{1}{F_L - F^0} \quad (1)$$

Where [A] represents the analytical concentration of GMF, F<sup>0</sup> and F are the fluorescence intensities in the absence and presence of GMF, respectively,

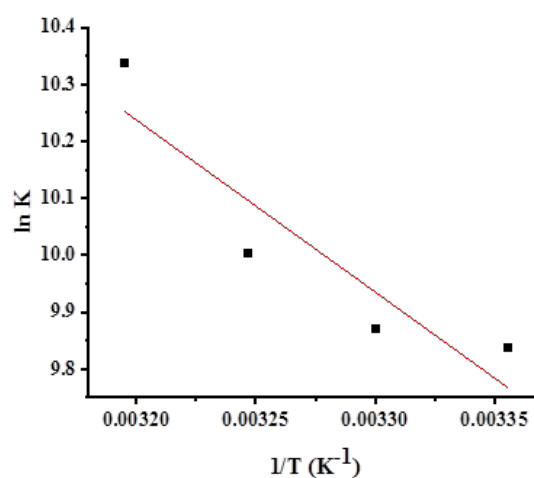


Table 1: Binding constants for the interaction of Tb(III)-(AZ)<sub>2</sub> with GMF

Temp. (K)	Stoichiometry suggested	Intercept	Slope	K (l mol <sup>-1</sup> )	R <sup>2</sup>
298	1:1	-2.06x10 <sup>-5</sup>	1.10x10 <sup>-9</sup>	18.73x10 <sup>3</sup>	0.989
303	1:1	-2.44x10 <sup>-5</sup>	1.26x10 <sup>-9</sup>	19.37x10 <sup>3</sup>	0.991
307	1:1	-4.02x10 <sup>-5</sup>	1.82x10 <sup>-9</sup>	22.09x10 <sup>3</sup>	0.992
313	1:1	-1.21x10 <sup>-4</sup>	3.92x10 <sup>-9</sup>	30.87x10 <sup>3</sup>	0.991

Figure 10: Hypothesized structure of Tb(III)-(AZ)<sub>2</sub>-GMF

### 3.2.6. Thermodynamic parameters and nature of the binding forces

Figure 11: Van 't Hoff plot for the Tb(III)-(AZ)<sub>2</sub>-GMF complex in methanol

$F_L$  is the limiting intensity of fluorescence and  $\alpha$  is  $1/F_L - F^0$ , and  $K$  is the binding constant between Tb(III)-(AZ)<sub>2</sub> probe and GMF which can be evaluated from the slope and intercept ( $K = \text{intercept/slope}$ ).

A plot of  $\frac{F^0}{F - F^0}$  versus  $1/[A]$  according to equation (1) was drawn and the data are presented graphically as shown in Figure (9). A good linear relationship is obtained ( $r^2=0.992-0.989$ ). This suggests that stoichiometry of the formed Tb-(AZ)<sub>2</sub> complex with GMF is 1:1, as shown in Table (1). The high value of the association constants indicates that the forming Tb-(AZ)<sub>2</sub>-GMF complex is highly stable. It is likely that the two vacant co-ordination sites of the terbium ion coordinate with GMF via its keto and carboxylate groups. Therefore, a proposed structure of the Tb(III)-complex is shown in Figure (10).

Table 2: Thermodynamic parameters for the interaction of Tb(III)-(AZ)<sub>2</sub> with GMF

T (K)	K (l mol <sup>-1</sup> )	$\Delta H$ (kJ mol <sup>-1</sup> )	$\Delta S$ (J mol <sup>-1</sup> K <sup>-1</sup> )	$\Delta G$ (kJ mol <sup>-1</sup> )
298	18.73x10 <sup>3</sup>			-24.37
303	19.37x10 <sup>3</sup>			-24.87
308	22.09x10 <sup>3</sup>	25.13	165.54	-25.61
313	30.87x10 <sup>3</sup>			-26.90

The thermodynamic parameters associated with temperature variation were analyzed to further characterize the binding forces between the Tb-(AZ)<sub>2</sub> complex and GMF in methanol. Since the fluorescence spectra demonstrated that the interaction between Tb-(AZ)<sub>2</sub> complex and GMF do

exist, it is necessary to further determine which kind of driving forces exist in the binding process. The enthalpy and entropy for the reactions were evaluated from the corresponding  $\ln K$  at different temperatures by applying the Van 't Hoff equation:

$$\ln K = -\Delta H/RT + \Delta S/R \quad (2)$$

$$\Delta G = -RT \ln K \quad (3)$$

where  $T$  is the experimental temperature (Kelvin),  $R$  is the gas constant, and  $K$  is the binding constant at the related temperature.  $\Delta H$  and  $\Delta S$  are enthalpy and entropy change of the reaction, respectively.  $\Delta G$  is free energy change.

A plot of  $\ln K$  versus  $1/T$  for the Tb-(AZ)<sub>2</sub>-GMF complex was obtained as shown in Figure (11), the enthalpy and entropy of this system were determined from the slope and intercept, respectively. The results obtained are presented in Table (2).

The reaction of the Tb-(AZ)<sub>2</sub> complex with GMF is spontaneous as indicated from the negative value for  $\Delta G$ . The positive value of the enthalpy ( $\Delta H$ ) indicates that the formation of the Tb-(AZ)<sub>2</sub> complex with GMF was an endothermic reaction. The positive  $\Delta H$  and  $\Delta S$  were attributed to hydrophobic interactions being the primary contributor to the binding [36, 37].

### 3.3. Calibration curve and limit of detection for GMF

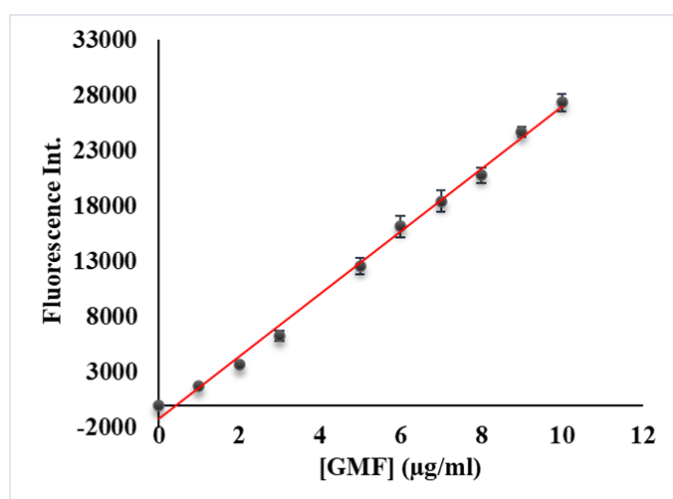


Figure 12: Calibration plot of the determination of GMF in the microtiter plate (error bars indicate standard deviations of five replicates)

Table 3: Linear range, regression equation, correlation coefficients, RSDs and LODs for determination of GMF in the microtiter plate

Parameter	Value
Regression equation	$Y=2820X - 1198$
slope	2820
intercept	-1198
$R^2$	0.9953
Accuracy	$97.79 \pm 6.20$
Correlation coefficient (r)	0.9976
linear range ( $\mu\text{g}/\text{mL}$ )	0.15-10
SE of intercept	13.78
SD of intercept	43.58
LOQ ( $\mu\text{g}/\text{mL}$ )	0.15
LOD ( $\mu\text{g}/\text{mL}$ )	0.05
RSD%	6.34
RE%	4.43

The method shows a linear calibration plot in the concentration range of 0.15-10  $\mu\text{g}/\text{mL}$  ( $3.1 \times 10^{-7}$  -  $2.1 \times 10^{-5}$  mol/L) of GMF (Figure 12). Linear regression yields the following equation:  $Y = 2820X - 1198$  ( $r = 0.9976$ ), where  $Y$  is the average fluorescence intensity and  $X$  is the concentration of GMF in  $\mu\text{g}/\text{mL}$ . Further analytical figures of merit of the calibration data are given in Table (3). The LOD was calculated to be 0.05  $\mu\text{g}/\text{mL}$  ( $1.0 \times 10^{-7}$  mol/L). The LOQ of the proposed method is 0.15  $\mu\text{g}/\text{mL}$  ( $3.1 \times 10^{-7}$  mol/L). The results of intraday repeatability, expressed as the relative standard deviation (RSD) are shown in table (4), and were found to be 0.38, 2.55, 2.63 and 3.38 % for the concentrations of 1.0, 5.0, 6.0 and 8.0  $\mu\text{g}/\text{mL}$ , respectively. Furthermore, the analysis of GMF standard solutions on two different days showed adequate values of precision ( $\text{RSD} \leq 5\%$  for each concentration) considering the mean fluorescence intensity values **Table (4)**. Accuracy of the method was expressed in terms of deviation (in %) of the mean calculated concentrations from the actual concentrations of the GMF standard solutions (1.0, 5.0, 6.0 and 8.0  $\mu\text{g}/\text{mL}$ ) **Table (4)**. Since the results were within the acceptable range of about  $\pm 5\%$ , the method is deemed to be accurate. The mean recoveries over two days were found to be 99.25 %, 98.17 %, 106.89 % and 98.93 %, respectively.

Table 4: Intraday and interday repeatability of the quantitation of Gemifloxacin mesylate in the microtiter plate (n = 5).

Parameters	Intraday concentration of GMF ( $\mu\text{g/mL}$ )				Interday concentration of GMF ( $\mu\text{g/mL}$ )			
	1	5	6	8	1	5	6	8
Fluorescence Int.	Day 1	Day 1	Day 1	Day 1	Day 2	Day 2	Day 2	Day 2
	1785	12775	15980	20716	1759	12695	14900	20152
	1800	13000	16487	21163	1720	12100	15912	20985
	1788	12951	16880	21437	1655	11980	16987	20256
	1799	13148	16700	20983	1698	11989	16856	19785
	1790	12300	15911	19616	1790	12003	16152	19616
mean	1792.4	12834.8	16391.6	20783	1724.4	12153.4	16161.4	20158.8
SD a	6.73	327.3	431	703.3	52.52	306.6	839.3	530.7
RSD% b	0.38	2.55	2.63	3.38	3.05	2.52	5.19	2.63
Recovery%	99.2	100.77	105.69	99.39	99.25	98.17	106.89	98.93
RE% c	0.8	0.77	5.69	0.61	0.75	1.83	6.89	1.07
Found $\pm$ SD	0.99 $\pm$ 0.002	5.04 $\pm$ 0.12	6.34 $\pm$ 0.16	7.95 $\pm$ 0.26	0.99 $\pm$ 0.02	4.90 $\pm$ 0.12	6.41 $\pm$ 0.32	7.91 $\pm$ 0.20

<sup>a</sup>SD Standard deviation <sup>b</sup>RSD Relative standard deviation (RSD (%) = (SD / mean)  $\times$  100)<sup>c</sup>RE (%) = (Actual concentration - Mean calculated concentration) / Actual concentration  $\times$  100

**Table (5)** summarizes the figures of merit of common methods for determination of GMF in particular analytical ranges, LODs, and specific features. All methods show reasonable linear ranges towards the assay of GMF. Tb(III)-(AZ)<sub>2</sub> complexes represent promising new fluorescent probes that display specific advantages over established procedures for GMF determination. The proposed methods show a narrower linear range than some other techniques, but it is simpler to perform and more rapid. The main advantages of the lanthanide probes include the use of the emission at longer wavelengths, the use of the long lag times and the large Stokes shifts which can be used to alleviate the scattering interference and the background autofluorescence from biological samples. GMF contains  $\alpha$ -keto-acid functionality that could chelate with lanthanide ions and acts as an antenna to transfer its emission energy to the lanthanide ion. This sensitized emission with a large Stokes' shift and narrow emission band in the longer wavelength region is expected to enable to detect GMF in biological samples without any sample preparation or pretreatment procedures. While the previously reported techniques such as chromatography [2] and capillary zone electrophoresis [9] have certain drawbacks, including the use of large quantities of solvent, requiring high technical skills and a long time for detection. On the other hand, the electrochemical methods [38] showed a wider linear range than the other methods. The proposed luminescent method, Tb(III)-(AZ)<sub>2</sub> probe shows a competitive detection limit. In addition, it is performed in a high-throughput microtiter plate format where 96 samples are detected within 2 minutes which is a huge advantage compared to chromatographic and electrophoretic methods. Also, its statistically robust data can be easily obtained because microplates enable up to 12 replicate measurements of each sample with a total volume not higher than required for one measurement in a 1 cm cell. Finally, this method can be considered as the first method for determination of GMF using a time-resolved luminescence technique.

Table 5: Figures of merit of selected methods for determination of GMF

Method	Linear range ( $\mu\text{g/mL}$ )	LOD ( $\mu\text{g/mL}$ )	Sampling time	Comments	Ref.
potentiometry	$2.43 \times 10^{-3}$ -4850	0.07	31 hours	31 hours for derivatization	[38]
HPLC	0.5-150	0.40	10 min.	10 min. for derivatization	[39]
spectrophotometry	5-27	4.49	15 min.	45 min. for derivatization	[40]
capillary zone electrophoretic	20-80	1.0	3 min	72 min for derivatization	[41]
Anodic Voltametric	0.24 – 4.85	0.07	5 min.	5 min. for derivatization	[42]
Fluorometry	0.5-4.0	0.04	5 min	40 min incubation	[43]
Luminescence in microtiter plate using Tb(III)-(AZ) <sub>2</sub>	0.15-10	0.05	3 min for 96 samples	2 min for data readout	[Present work]

Table 6: Recovery of GMF in different pharmaceutical samples and in human plasma as determined by luminescence

Formulation studied	Amount of pure drug (Gemifloxacin mesylate) added ( $\mu\text{g/ml}$ )	Total found ( $\mu\text{g/ml}$ )	Recovery% $\pm$ SD a
Floxguard tablet(399mg)	0	1.10	.
	3	4.17	101.71 $\pm$ 3.37
	5	6.26	102.62 $\pm$ 0.66
	7	8.29	102.35 $\pm$ 0.93
Gemionce tablet(399mg)	0	1.40	.
	3	4.72	107.27 $\pm$ 11.80
	5	6.41	100.16 $\pm$ 3.67
	7	8.49	101.07 $\pm$ 2.47
Quinabiotic tablet(400mg)	0	1.10	.
	3	4.26	103.90 $\pm$ 1.73
	5	6.04	99.02 $\pm$ 2.27
	7	8.45	104.32 $\pm$ 2.15
Human plasma	3	2.94	98.00 $\pm$ 3.25
	5	4.88	97.60 $\pm$ 1.36
	7	6.90	98.57 $\pm$ 2.32

<sup>a</sup>Mean of five determinations

### 3.4. Effect of interfering species on estimation of GMF using Tb(III)-(AZ)<sub>2</sub> complex

The luminescence response of the Tb(III)-(AZ)<sub>2</sub> complex was examined in the presence of both, various potential interferents (primarily as used in pharmaceutical formulations) and GMF antibiotic (5  $\mu\text{g/ml}$ ). The interferents studied were anhy-

drous lactose, Avicel PH101, talc, titanium dioxide, magnesium stearate, croscarmellose sodium salt, polyvinylpyrrolidone (PVP K30) and starch. The tolerance limit was set at the highest concentration of interferents yielding an inaccuracy of  $\pm 10.0\%$ . The results are summarized in Table (S1) and show no significant interference from excipients and ad-

ditives, indicating a high selectivity for determining the studied GMF in its dosage forms.

### 3.5. Determination of GMF in real samples

The proposed method was then used to determine the concentration of GMF in four real samples. Among them, there was one plasma sample from a healthy volunteer and three pharmaceutical tablet samples (Floxguard, Gemionce, and Quinabiotic). The samples were collected and were prepared as described in Section 2.3, and the concentration of GMF was determined using the Tb(III)-(AZ)<sub>2</sub>-probe as outlined in Section 2.4. The results are presented in Table (6). Furthermore, spiking GMF into the above mentioned diluted real samples yielded recoveries from 97.60% to 107.27%, with an average of 102.44% and relative standard deviations of less than 5%. So, the luminescence method works reliably and accurately. This suggests that no substantial interference occurred in such real samples. These findings demonstrate that the present luminescence method is capable of reliably detecting GMF in complex real pharmaceutical samples. So, the obtained results shown in Table (6) are satisfactorily accurate and precise.

## 4. Conclusion

The proposed fluorometric method could be successfully used for the determination of Gemifloxacin Mesylate in the pharmaceutical formulation. The proposed procedure is simple, sensitive, reliable, and rapid. It could be regarded as a useful technique for the routine quality control of pharmaceutical formulations with a relatively inexpensive instrumentation. In addition, the proposed method is very suitable to be applied in content uniformity testing.

## References

- [1] F. Zhao, H. Zhao, W. Xiong, Chemiluminescence determination of gemifloxacin based on diperiodatoargentate (III)-sulphuric acid reaction in a micellar medium, *Luminescence* 28 (2013) 108–113.
- [2] M. Rudrapal, N. Hussain, Method development and validation of gemifloxacin in tablet dosage form by RP-HPLC, *J. Drug Deliv. Ther* 10 (2020) 97–101.
- [3] S. Yıldırım, H. Karakoç, A. Yaşar, İ. Determination of levofloxacin, ciprofloxacin, moxifloxacin and gemifloxacin in urine and plasma by HPLC-FLD-DAD using pentafluorophenyl core-shell column: Application to drug monitoring, *Biomed. Chromatogr* 34 (2020).
- [4] M. Kiyimaci, A. Gumustas, M. Gumustas, A. Akin, S. Ozkan, Comparative study for the determination of gemifloxacin by HPLC and microbiological methods from pharmaceutical preparations and biological samples, *Curr. Pharm. Anal* 11 (2015) 193–200.
- [5] S. Mousavi, Determination of gemifloxacin in human plasma by high performance liquid chromatography using Ultra Violet detector and its application to a bioequivalence study, *Brazilian J. Pharm. Sci* 54 (2019).
- [6] B. Roy, A. Das, U. Bhaumik, A. Sarkar, A. Bose, J. Mukharjee, U. Chakrabarty, A. Das, T, Determination of gemifloxacin in different tissues of rat after oral dosing of gemifloxacin mesylate by LC-MS/MS and its application in drug tissue distribution study, *J. Pharm. Biomed. Anal* 52 (2010) 216–226.
- [7] E. Doyle, S. Fowles, D. McDonnell, R. McCarthy, S. White, Rapid determination of gemifloxacin in human plasma by high-performance liquid chromatography-tandem mass spectrometry, *J. Chromatogr. B Biomed. Sci. Appl* 746 (2000) 333–342.
- [8] R. Zhao, Q. Wang, X. Hu, T. Nie, X. Yang, C. Li, X. Lu, X. Wang, J. Jiang, J. Pang, X. You, Microdialysis combined with liquid chromatography-tandem mass spectrometry for the quantitation of gemifloxacin and its application to a muscle penetration study in healthy and MRSA-infected rats, *PLoS One* 14 (2019).
- [9] A. Elbashir, B. Saad, A. Ali, K. Al-Azzam, H. Aboul-Enein, Validated stability indicating assay of gemifloxacin and lomefloxacin in tablet formulations by capillary electrophoresis, *J. Liq. Chromatogr. Relat. Technol* 31 (2008) 1465–1477.
- [10] S. Al-Tamimi, A. Al-Mohaimeed, N. Alarfaj, F. Aly, Electrochemical determination of gemifloxacin mesylate in commercial tablets and biological fluids by differential pulse polarography, *Int. J. Electrochem. Sci* 15 (2020) 8386–8396.
- [11] S. Ali, A. Hassan, M. Muhammad, Cyclic voltammetric studies of gemifloxacin using gold electrode in presence of britton-robinson buffer, *Pak. J. Pharm. Sci* 31 (2018) 473–479.
- [12] Z. Xu, S. Han, C. Lee, J. Yoon, D. Spring, Development of off-on fluorescent probes for heavy and transition metal ions, *Chem. Commun* 46 (2010) 1679–1681.
- [13] B. Lü, Y. Chen, P. Li, B. Wang, K. Müllen, M. Yin, Stable radical anions generated from a porous perylene-dimide metal-organic framework for boosting near-infrared photothermal conversion, *Nat. Commun* 10 (2019) 767–775.
- [14] F. Faridbod, M. Ganjali, M. Hosseini, Lanthanide materials as chemosensors, Elsevier, 2018.  
URL <https://doi.org/10.1016/B978-0-12-813840-3>.

00012-0

- [15] D. Wu, A. Sedgwick, T. Gunnlaugsson, E. Akkaya, J. Yoon, T. James, Fluorescent chemosensors: The past, present and future, *Chem. Soc. Rev* 46 (2017) 7105–7123.
- [16] I. Hemmilä, V. Laitala, Progress in lanthanides as luminescent probes, *J. Fluoresc* 15 (2005) 529–542.
- [17] J. Lehn, Perspectives in supramolecular chemistry—from molecular recognition towards molecular information processing and self-organization, *Angew. Chemie Int. Ed. English* 29 (1990) 1304–1319.
- [18] B. Xu, H. Zhu, B. Yan, Novel langmuir-blodgett film with ternary europium complex of long chain mono-eicosyl cis-butene dicarboxylate and 1,10-phenanthroline: Cooperative assembly and luminescence, *Inorg. Chem. Commun* 13 (2010) 1448–1450.
- [19] Z. Ahmed, K. Iftikhar, Solution studies of lanthanide (III) complexes based on 1,1,1,5,5,5-hexafluoro-2,4-pentanedione and 1,10-phenanthroline Part-I: synthesis, <sup>1</sup>H NMR, 4f-4f absorption and photoluminescence, *Inorganica Chim. Acta* 363 (2010) 2606–2615.
- [20] A. Bencini, V. Lippolis, Phenanthroline: a versatile building block for the construction of ligands for various purposes, *Coord. Chem. Rev* 1 (2010) 2096–2180.
- [21] C. Xu, Photophysical properties of a new ternary europium complex with 2-thenoyltrifluoroacetone and 5-nitro-1,10-phenanthroline, *J. Rare Earths* 28 (2010) 60229–60234.
- [22] Y. Zhou, L. Zhou, J. Wu, H. Li, Y. Zheng, X. You, H. Zhang, Photo/electroluminescence properties of an europium (III) complex doped in 4,4'-N,N'-dicarbazole-biphenyl matrix, *Thin Solid Films* 518 (2010) 4403–4407.
- [23] V. Tsaryuk, K. Zhuravlev, A. Vologzhanina, V. Kudryashova, V. Zolin, Structural regularities and luminescence properties of dimeric europium and terbium carboxylates with 1,10-phenanthroline (C.N.=9), *J. Photochem. Photobiol. A Chem* 211 (2010) 7–19.
- [24] P. Sammes, G. Yahioglu, Modern bioassays using metal chelates as luminescent probes, *Nat. Prod. Rep* 13 (1996) 1–28.
- [25] M. Kaczmarek, Lanthanide-sensitized luminescence and chemiluminescence in the systems containing most often used medicines; a review, *J. Lumin* 222 (2020) 117–174.
- [26] J. Sousa, G. Alves, A. Fortuna, A. Falcão, Analytical methods for determination of new fluoroquinolones in biological matrices and pharmaceutical formulations by liquid chromatography: A review, *Anal. Bioanal. Chem* 403 (2012) 93–129.
- [27] H. Azab, G. Khairy, N. El-Ghany, M. Ahmed, A new luminescent bio-probe of Europium(III)-complex for sensing some biomolecules and CT-DNA, *J. Photochem. Photobiol. A Chem* 374 (2019) 1–9.
- [28] E. Moore, A. Samuel, K. Raymond, From antenna to assay: lessons learned in lanthanide luminescence, *Acc. Chem. Res* 42 (2009) 542–552.
- [29] J. Streeton, N. Desem, S. Jones, Sensitivity and specificity of a gamma interferon blood test for tuberculosis infection, *Int. J. Tuberc. Lung Dis* 2 (1998) 443–450.
- [30] W. Vosburgh, G. Cooper, Complex ions. I. the identification of complex ions in solution by spectrophotometric measurements, *J. Am. Chem. Soc* 63 (1941) 437–442.
- [31] J. Lehn, Supramolekulare chemie - moleküle, übermoleküle und molekulare funktionseinheiten (nobel-vortrag), *Angew. Chemie* 100 (1988) 91–116.
- [32] R. Anderson, D. Bendell, P. |groundwater, *Organic spectroscopic analysis* 22 (2004).
- [33] R. Pratiwi, A. Nandiyanto, How to read and interpret uv-vis spectrophotometric results in determining the structure of chemical compounds, *Indones. J. Educ. Res. Technol* 2 (2022) 1–20.
- [34] E. Geladé, F. De Schryver, Energy transfer in inverse micelles, *J. Am. Chem. Soc* 106 (1984) 5871–5875.
- [35] J. Ocaña, F. Barragán, M. Callejón, Fluorescence and terbium-sensitized luminescence determination of garenoxacin in human urine and serum, *Talanta* 63 (2004) 691–697.
- [36] P. Ross, S. Subramanian, Thermodynamics of protein association reactions: forces contributing to stability, *Biochemistry* 20 (1981) 3096–3102.
- [37] Y. Zhang, X. Chen, J. Dai, X. Zhang, Y. Liu, Y. Liu, Spectroscopic studies on the interaction of lanthanum(III) 2-oxo-propionic acid salicyloyl hydrazone complex with bovine serum albumin, *Luminescence* 23 (2008) 150–156.
- [38] M. Idress, A. Elbashir, Development and validation of potentiometric ZnO nanorods modified ion selective electrode for determination of gemifloxacin in pharmaceutical formulation, *Curr. Trends Anal. Bioanal. Chem* 1 (2017) 50–56.
- [39] H. Ali, S. M. T. Rafi, S. Ikram, F. Zafar, S. Naeem, E. Zaheer, N. Mallick, S. Khan, A. Nawab, A. Tariq, Gemifloxacin mesylate determination in raw material, dosage form and human plasma: An application to in vivo analysis, *Lat. Am. J. Pharm* 39 (2020) 1725–1733.
- [40] D. Zidan, O. Ismaiel, W. Hassan, A. Shalaby, Simple spectrophotometric and conductometric methods for determination of gemifloxacin in pure, pharmaceutical dosage form and human urine, *J. Appl. Pharm. Sci* 6 (2016) 136–143.
- [41] C. S. Paim, F. Führ, V. Todeschini, M. Steppe, E. E. Scherman, Schapoval, Simultaneous analysis of gemifloxacin mesylate and its main synthetic impurity by an optimized capillary zone electrophoretic method, *Anal. Methods* 6 (2014) 1657–1665.
- [42] A. E. Radi, A. Khafagy, A. El-Shobaky, H. El-Mezayen, Anodic Voltammetric determination of gemifloxacin using screen-printed carbon electrode, *J. Pharm. Anal* 3 (2013) 132–136.
- [43] A. M. El-Didamony, M. O. Abo-Elsoad, Spectrofluorimetric and spectrophotometric methods for the determination of gemifloxacin in bulk and tablets, *Main Gr. Chem* 14 (2015) 59–70.